

DETC2016-59940

SURFACE ERROR AND STABILITY CHART OF BEAM-TYPE WORKPIECE IN MILLING PROCESSES

Adam K. Kiss

Department of Applied Mechanics
Budapest University of
Technology and Economics
Budapest, Hungary
Email: kiss_a@mm.bme.hu

Daniel Bachrathy

Department of Applied Mechanics
Budapest University of
Technology and Economics
Budapest, Hungary
Email: bachrathy@mm.bme.hu

Gabor Stepan

Department of Applied Mechanics
Budapest University of
Technology and Economics
Budapest, Hungary
Email: stepan@mm.bme.hu

ABSTRACT

In milling processes, the intermittent cutting force may lead to harmful vibrations. These vibrations are classified into two groups. One of them is the self excited vibration which comes from the loss of stability due to the regeneration effect and these vibrations lead to unacceptable chatter marks. The other one is the forced vibration which can lead to high Surface Location Error (SLE) in case of resonant spindle speeds. In this paper, the dynamics of the beam-type workpiece is considered which is modelled by means of Finite Element Analysis (FEA). Both the forced vibration and the stability properties are predicted along the tool path. The surface properties are computed on the stable regions of the stability chart which presents the chatter-free (stable) parameter domain as a function of the spindle speed and the tool path. The theoretical results are compared to the measured SLE and surface roughness.

1 INTRODUCTION

Eliminating the vibrations during milling process is an important task, but unfortunately, it is unattainable in practice. The reason for this is two different types of vibration, which may occur during the process. One of them is the self-excited vibration that is due to the loss of stability related to the surface regeneration effect [1]. The chip evolution is influenced by the subsequent position of the previous cutting edge and the current position of the current cutting edge [2]. This effect can be modelled with

delay-differential equations (DDE) [3]. The other type of vibration is the periodic forced vibration, but it plays a role only in the case if the machining process is stable. The forced vibration can be described by simple inhomogeneous ordinary differential equation (ODE) and it leads to large amplitude vibration in resonant cases. From the mechanical point of view, the machining process is usually stable if the spindle frequency is close to the natural frequencies or its higher harmonics, however, large amplitude resonant vibration can occur at these spindle speeds. The relative vibration between the milling tool and the workpiece results a deviation between the machined and the desired surface, which also called as the Surface Location Error (SLE) [4, 5].

It is an essential role for a mechanical engineer to predict the behaviour of a milling process in order to achieve high material removal rate, thus increase the production rate in manufacturing. The stability properties is usually determined based on the so-called stability chart which presents the domain of the chatter-free (stable) technological parameter domain. It is usually represented in the plane of the spindle speed and the axial immersion. It can be calculated by means of methods in time domain [6–8] or frequency domain also [9–11]. In time domain, the identification of the modal parameters - which describe the dynamical behavior of the model - is required but it is complex engineering procedure. An advantage of the frequency domain solutions is that they can directly use the measured Frequency Response Function (FRF). However, these FRF functions change in the work-space due to the different configuration of the machine tool

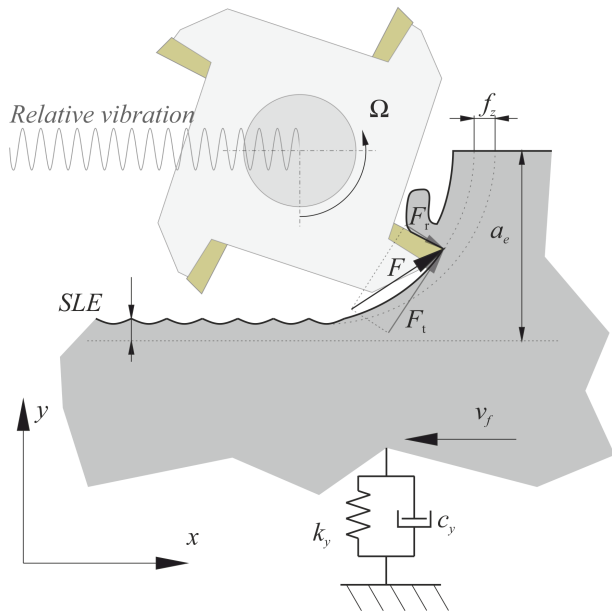


FIGURE 1. Dynamic model of the milling tool.

structure. The variation of the FRF is even more significant if the dynamics of the workpiece is dominant (i.e.: flexible workpiece compared to the milling tool, which is typical for beam-type or thin plate-type workpieces). From the viewpoint of the stability chart calculation, it is essential to take into account the effect of the variation in the FRF function.

In this paper, stability chart and surface properties (SLE) calculations are developed using an FRF based model. The variation of the dynamic properties caused by the material removal and the changing milling tool position is also considered. Finally, the predicted phenomena are identified in measurement results.

2 MILLING PROCESS

In order to perform the stability calculation and to predict the milled surface quality, the cutting process of the milling operation has to be described. In this paper, the widespread linear force model is used, where the magnitude of the cutting force is linearly proportional to the actual chip thickness [12]. This is a good approximation for the computation of the forced vibration [13] and acceptable to describe the chatter phenomenon [14]. The ratios described by the K_r radial and the K_t tangential cutting coefficients, which usually determined by set of cutting tests for a given tool geometry and cutting parameters [15].

The tangential and the radial component of the elementary cutting forces acting on an elementary segment of the j^{th} cutting

edge dz can be described according to [16]

$$dF_r(t) = K_r g(\varphi_j(t, z)) h(\varphi_j(t, z)) dz \cos \eta, \quad (1)$$

$$dF_t(t) = K_t g(\varphi_j(t, z)) h(\varphi_j(t, z)) dz \cos \eta, \quad (2)$$

where $g(\varphi_j(t, z))$ is the screen function

$$g(\varphi_j(t, z)) = \begin{cases} 1 & \text{if the tool is in the material} \\ 0 & \text{otherwise} \end{cases} \quad (3)$$

which indicates that the j^{th} edge is in contact with the material or not, $\varphi_j(t, z)$ is the current angular position of the j^{th} cutting edge (which depends on the axial coordinate of the tool z), reads as

$$\varphi_j(t, z) = \Omega t + \frac{2\pi(j-1)}{N} - \frac{2\pi z}{p} \quad (4)$$

for constant helix angle and equally distributed teeth, where N is the number of the cutting edges, Ω is the angular spindle speed in [rad/s] and p is the helix pitch. $\eta = \arctan D\pi/(Np)$ is the helix angle and $h(\varphi_j(t, z))$ is the chip thickness. It is the sum of the dynamic chip thickness $h_{\text{dyn}}(\varphi_j(t, z))$ and the stationary chip thickness $h_{\text{stat}}(\varphi_j(t, z))$ [6]. The stationary one is the result of the projection of the feed per tooth f_z on the direction of the tool tip velocity, reads as

$$h_{\text{stat}}(\varphi_j(t, z)) = f_z \sin \varphi_j(t, z). \quad (5)$$

Note, that the stationary chip thickness influences only the forced vibration, and it has no effect on the stability if linear cutting force is considered as in Eq. (1,2) [4]. The dynamic one corresponds to the surface regenerative effect of the machining process [9] which plays a role in the stability analysis of the forced periodic motion [17].

$$h_{\text{dyn}}(\varphi_j(t, z)) = (y(t, z) - y(t - \tau, z)) \cos \varphi_j(t, z) \quad (6)$$

where $y(t)$ is the general coordinate, which describes the relative motion between the workpiece and the milling tool (see in Fig. 1) and τ is the tooth passing period ($\tau = 2\pi/(\Omega N)$).

To determine the resultant cutting force, first, the radial and tangential cutting force components are projected from the local tangential-radial coordinate system of the j^{th} tooth to the global $x - y$ coordinate system. Then it is integrated along the axial coordinate z from zero to the axial immersion a_p .

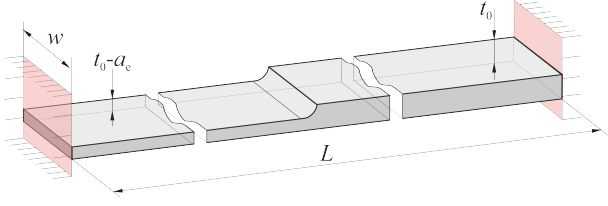


FIGURE 2. Schematic figure of the applied beam-type workpiece considering the material removal

$$F_y(t) = \sum_{j=1}^N \int_0^{a_p} [K_t \ K_r] h(\varphi_j(t, z)) g(\varphi_j(t, z)) [-\sin \varphi_j(t, z) \ \cos \varphi_j(t, z)]^T dz \quad (7)$$

Note, that the *SLE* computation requires the forced vibration perpendicular to the surface, therefore only the $F_y(t)$ component is presented in Eq. (7) and the motion is restricted to the direction perpendicular to the machined surface.

With the previously described cutting force model, the stability and surface quality calculation can be performed after the dynamic behaviour of the model is described.

3 DYNAMICS OF THE WORKPIECE

In this paper, the workpiece is assumed much more flexible compared to the the milling tool together with the whole machine tool structure. This assumption is valid for a thin walled workpiece, for example Fig. 2. The milling tool and the workpiece are considered as a rigid body and a flexible body, respectively.

During the milling process, the actual tool position along the tool path defines the contact region between the milling tool and the workpiece. Due to this phenomenon, different points are excited by the resultant cutting force, hence the dynamic behavior at the actual contact point needs to be considered during the computation. It can be easily provide by means FEA. In case of a given workpiece geometry, the corresponding modal matrices can be extracted from most of the industrial FEA softwares. Our assumption for the geometry is that the transversal dimensions (thickness and width) are negligible compared to the longitudinal size ($t_0 \ll w \ll L$), as shown in Figure 2. In this case, the horizontal (longitudinal) vibration is not taken into consideration, since the structure is much more stiffer in the horizontal direction compared to the transversal direction. Furthermore, if the width of the plate w is small, then the resultant bending moment along the workpiece length L is also small, therefore its effect can be also neglected. Due to these assumptions the bending vibration is dominant in the model, thus, for the sake of simplicity, a simple beam model is considered and described by Finite

Element Analysis in this paper, which capable of describing all phenomena in question.

The workpiece dynamics can change during the milling process in two different ways. One of them corresponds to the movement of the excitation position, which is taken into account by means of the mode shapes. The other one relates to the effect of the material removal process, which leads to changing workpiece geometry and changing dynamical parameters, especially the natural frequency.

The governing equation of motion can be given as decoupled equations of each modal coordinates $\chi_i(\omega, s)$ in frequency domain [18, 19], read as

$$-\omega^2 \chi_i(\omega, s) + i\omega 2\xi_i(s) \omega_{n,i}(s) \chi_i(\omega, s) + \omega_{n,i}^2(s) \chi_i(\omega, s) = \phi_i(\omega), \quad (8)$$

where $\phi_i(\omega)$ is the generalized force of i^{th} mode shape, s describe the arc length coordinate of the tool path (which is equivalent to the beam length coordinate), $\omega_{n,i}(s)$ is the natural angular frequency and $\xi_i(s)$ is the modal damping of the i^{th} mode shapes, ($i = 1, 2, \dots, m$, where m is the number of the considered modes). In case of proportional damping, damping coefficients $\xi_i(s)$ can be calculated as:

$$\xi_i(s) = \frac{\alpha_M}{2\omega_{n,i}(s)} + \frac{\alpha_K}{2} \omega_{n,i}(s), \quad (9)$$

where α_M and α_K are the proportional damping factors [18]. With a FEA based model, the variation of the FRF can be modelled for each node of the FEA model. The FRF $H(\omega, s)$ in the function of the frequency ω and the tool position s at the contact milling point of the tool and workpiece can be given as

$$H(\omega, s) = \sum_{i=1}^m \frac{T_{\text{exc},i}^2(s)}{-\omega^2 + i\omega 2\xi_i(s) \omega_{n,i}(s) + \omega_{n,i}^2(s)}, \quad (10)$$

where $T_{\text{exc},i}(s)$ is the element of the i^{th} mass normalized mode shape vector at the excited contact milling point [18], as shown in Fig. 3.

4 SURFACE LOCATION ERROR

In this section, the computation steps of the forced vibration induced *SLE* are presented based on [5]. The machined surface contour is defined by the relative motion of the cutting edges and the excited contact point of the vibrating workpiece. The forced periodic vibration of the contact point can be defined based on the given FRF $H(\omega, s)$ (Eq. 10) as:

$$y(t, s) = \mathcal{F}^{-1}(H(\omega, s) \phi_y(\omega)), \quad (11)$$

Parameter	Symbol	Workp. I.	Workp. II.
Width	w	15 [mm]	20 [mm]
Thickness	t_0	3 [mm]	5 [mm]
Length	L	100 [mm]	
Density	ρ	2933.33 [$\frac{kg}{m^3}$]	
Young's modulus	E	50 [GPa]	
Material	-	AlMgSi05	

TABLE 1. Parameters of the milled workpieces (Workp. I. and II.)

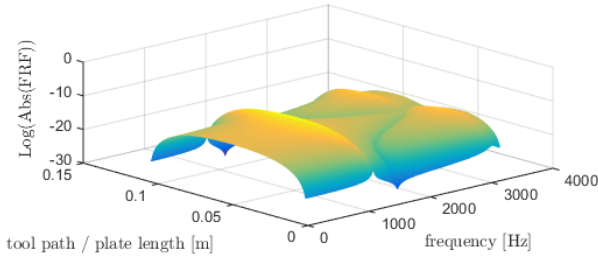


FIGURE 3. Frequency Response Function of the workpiece depending on the length of the workpiece, where only the first two modes are taken into account ($m = 2$). Parameters are presented in Table 1.

where $\phi_y(\omega)$ is the Fourier Transformation of Eq. 7. The relative motion of the cutting edge is formulated as the superposition of the forced stationary vibration $y(t, s)$ and the cylindrical rotation of the edge:

$$r_j(t, s, z) = y(t, s) - \frac{D}{2} \cos \phi_j(t, z). \quad (12)$$

According to [5], the maximum of the relative displacement determines the *SLE*, which is given by

$$\begin{aligned} \text{Up-milling: } SLE(s, z) &= \max_t(r_j(t, s, z)) - \frac{D}{2} \\ \text{Down-milling: } SLE(s, z) &= \min_t(r_j(t, s, z)) + \frac{D}{2}. \end{aligned} \quad (13)$$

Consequently, the $SLE(s, z)$ does not only depend on the tool path coordinate s , but also on the axial coordinates z . Therefore, the so-called *Maximum Surface Location Error MSLE(s)* surface quality parameter can be introduced, which is the maximum of the $SLE(s, z)$ function, reads as

$$MSLE(s) = \max_z(SLE(s, z)). \quad (14)$$

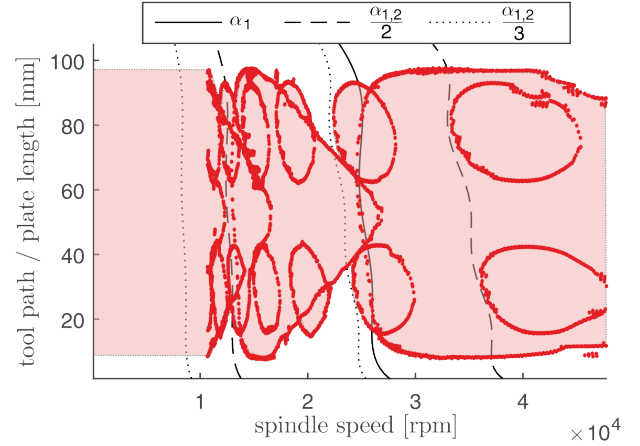


FIGURE 4. Stability diagram in the plane of the tool path s and the spindle speed Ω . The red dots show the bifurcation curves along which the stability properties changing and the light red shaded area represents the unstable region. Continuous, dashed and dotted lines represents the resonant spindle speeds referring to the first, second and third higher harmonics of the first two natural frequencies, respectively

The presented method can be used to predict the *MSLE* values along the tool path for a given set of technological parameters. However, since these computations are based on the stable forced vibration, it is valid only if the machining process is stable from the viewpoint of the regenerative effect.

5 STABILITY ANALYSIS

In what follows, the stability boundaries of the regenerative effect are presented based on the so-called Extended Multi Frequency Solution (EMFS) [11]. The EMFS is an efficient computational algorithm for determine the stability boundaries by means of to calculate the real and the imaginary parts of the determinant of the truncated Hill's infinite matrix. With the help of the EMFS, the stability of the machining process can be determined for a given parameter set. The stability chart is computed in the plane of the tool path s and the spindle speed Ω by means of the so-called Multi-Dimensional Bisection Method [20], which is a fast interval halving numerical algorithm. The combination of the EMFS and the MDBM provides an efficient and fast computational method, which is capable to determine the stability boundaries. In Fig. 4, the stability is computed for parameters presented in Table 1 and 2. Note, that the stability chart does not show the traditional lobe structure since the vertical axis is not the axial immersion a_p , but the tool path coordinate s .

6 A CASE STUDY

6.1 Numerical results

The above-described computation method is applied to a case study, in which, the peripheral milling of beam-type workpieces are performed. Note, that in this paper the entire width of the workpiece is milled, therefore the axial immersion a_p is equal to the width of the workpiece ($w = a_p$). During the calculation, the generated FRF presented in Fig. 3 and the technological parameters shown in Table 1 and 2 are used. The so-called superchart (Fig. 5 and 6) [21] presents the boundaries of the stability chart together with the *MSLE* values in the plane of the spindle speed Ω and the tool path coordinate s . It is well-known that if the natural frequencies of the system is excited by one of the Fourier components of the cutting force then it can lead to large resonant vibrations. Therefore, substantial *MSLE* values are evolved typically at the resonant spindle speeds ($\Omega = \omega_n/(kN), k = 1, 2, 3, \dots$). Nevertheless, in case of helical edged cutting tool, there exist so-called trivial and non-trivial appropriate axial immersions [5, 13], where no resonant vibration take place, therefore negligible *MSLE* can be achieved. The trivial appropriate axial immersion is formulated as

$$w = pk, \quad k \in \mathbb{N}. \quad (15)$$

Note, that for Eq. (15), the cutting edges cover a full periods $[0, k2\pi]$, therefore, constant cutting force is resulted independently from the spindle speed Ω . The non-trivial appropriate axial immersion is given as

$$w(\Omega) = \frac{\Omega}{\omega_n} pk, \quad k \in \mathbb{N} \quad (16)$$

for which no resonant vibration of the selected natural frequency is evolved.

Fig. 5 shows that the favorable parameter domains can be found (at the pockets) between the stability lobes near to the resonant spindle speeds or its higher harmonics ($\Omega \approx 11000, 21000, 45000$ rpm), where the chatter can be eliminated for the full length of the workpiece. On the other hand, these regions are not recommended from the viewpoint of the surface errors due to the resonant vibration (see Fig. 5). However, if the conditions for the trivial or the non-trivial appropriate axial immersion Eq. (15, 16) are fulfilled, then small *MSLE* values formed. For a given axial immersion, we can reformulate Eq. (16) to give a condition for the number i of the higher harmonics of the resonant spindle speed (Ω/i):

$$i = \frac{kp}{w}, \quad i, k \in \mathbb{N}. \quad (17)$$

Note, it can be fulfilled only if p/w is rational.

Parameter	Symbol	Value
Feed per tooth	f_z	0.05 [mm]
Number of teeth	N	4 [-]
Helix pitch	p	10 [mm]
Tool diameter	D	8 [mm]
Radial immersion ratio	a_e	0.05 [-]
Axial immersion	$a_p = w$	width of the workpiece
Radial force coeff.	K_r	$300 \cdot 10^6 \left[\frac{N}{m^2} \right]$
Tang. force coeff.	K_t	$800 \cdot 10^6 \left[\frac{N}{m^2} \right]$
Damping coeff. I.	α_M	$1.43 \cdot 10^{-6} \left[\frac{1}{s} \right]$
Damping coeff. II.	α_K	45.02 [s]

TABLE 2. Parameters of the case study

In the case study of Workpiece I. $p/w = 2/3$ and Eq. (17) holds for parameter pairs $[i, k] = [2, 3], [4, 6], [6, 9], \dots$. This means, that the every second (even) resonant spindle speeds lead to negligible *MSLE* values, and the odd ones create resonant vibration and large surface error, as shown in Fig. 5.

In the case study of Workpiece II. ($p/w = 1/2$), Eq. (17) is hold for parameter pairs $[i, k] = [1, 2], [2, 4], [3, 6], \dots$, therefore, non of the spindle speeds would lead to resonance. This case demonstrate a special case, where the axial immersion a_p is double of the helix pitch p , hence, this situation corresponds to the trivial appropriate axial immersion. Thus, the cutting force is constant, therefore, there is no vibration and the small *MSLE* determined by the static deformation, only (see Fig. 6).

6.2 Measurement results

Measurements are performed on both of Workpiece I. and II. based on the parameters presented in Table 1. and Table 2. The first measurement performed for Workpiece I. at $\Omega = 17000$ rpm, which is the first resonant spindle speed of the first natural frequency. Fig. 7 shows the measured surface profile of the workpiece at different heights along the tool path. The upper envelope of the curves defines the *MSLE* function. It can be seen, that the pattern of the *MSLE* along the length of the workpiece has similar form to the respective mode shape and does not show chatter marks as it predicted in Fig. 5.

Spindle speed $\Omega = 22000$ rpm (the second resonant spindle speed of the second natural frequency) is also tested for which only negligible *MSLE* values are measured as predicted based on Eq. (17). However, we find chatter marks around the peaks of the corresponding mode shape. This is represented by the measured surface roughness in Fig. 8. The reasons for this could be that the size of the two unstable islands are underestimated and the

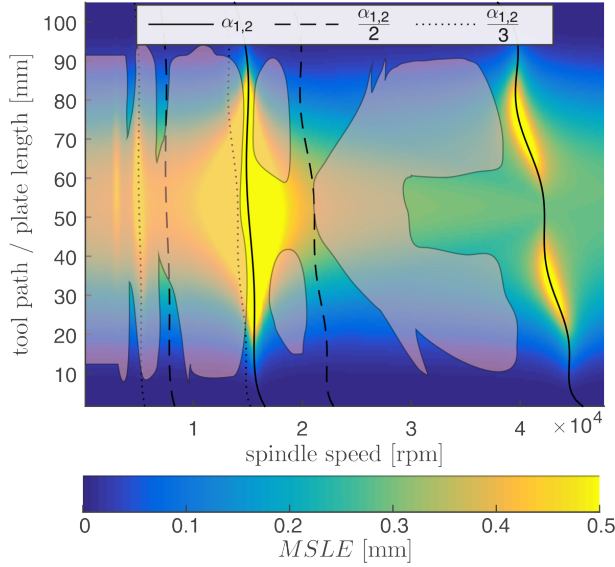


FIGURE 5. Maximum Surface Location Error and extended stability diagram in the function of the spindle speed along the tool path / plate length for up-milling for Workpiece I.; Parameters: $p = 10$ mm; $a_p = w = 15$ mm, $v = 3$ mm

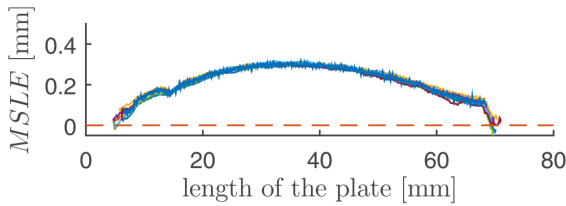


FIGURE 6. Measured $MSLE$ profile along the tool path for spindle speed $\Omega = 17000$ rpm; parameters from Table 1. and 2. for Workpiece I.

line of the selected spindle speed crosses them.

During the measurement performed for Workpiece II., we find chatter marks along the whole workpiece for all the tested spindle speeds as predicted by the numerical results in Fig. 6. As an example, the machined surface at $\Omega = 17000$ rpm is presented in Fig. 9, which shows chatter marks along the full length of the tool path. Note, that no shape deviation is detected, because trivial appropriate axial immersion (see Eq. $a_p = 2p$ is applied (15)).

CONCLUSION

In this study, it is shown that how the variation of the Frequency Response Function affect the stability and surface errors of the machining process. To demonstrate this phenomena, the workpiece is considered as a flexible body and its dynamic properties are assumed to be dominant compared to the machine tool.

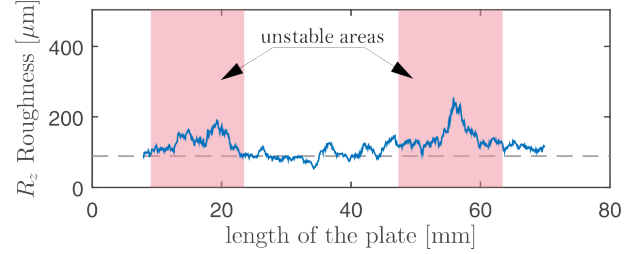


FIGURE 7. Measured Roughness for Workpiece I. at spindle speed $\Omega = 22000$ rpm, parameters from Table 1. and 2. High R_z values indicates the occurrence of chatter vibration

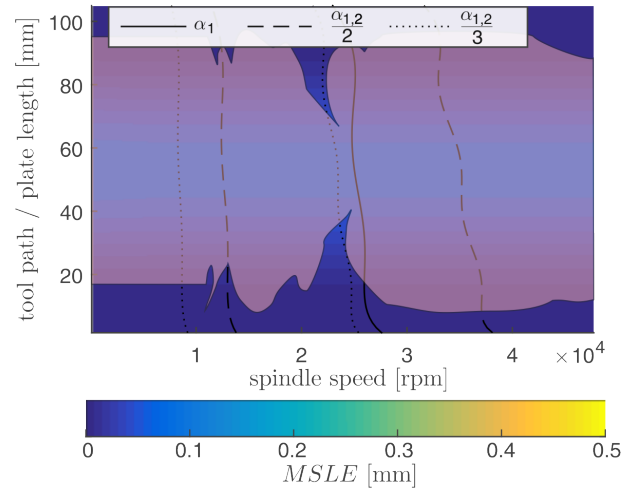


FIGURE 8. Maximum Surface Location Error and extended stability diagram in the function of the spindle speed along the tool path / plate length for down-milling for Workpiece II.; Due to the axial immersion is twice greater than the helix pitch, constant cutting force arises and only static deformation is occurred; Parameters: $p = 10$ mm; $a_p = w = 20$ mm, $v = 5$ mm

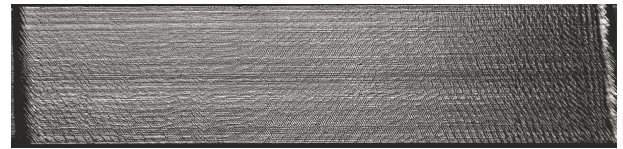


FIGURE 9. Chatter marks on the milled surface, parameters from Table 1 and 2 for Workpiece II. at $\Omega = 17000$ rpm

Furthermore, the changing stiffness caused by the material removal and the change in the position of the contact milling point are also considered. The stability boundaries together with the $MSLE$ values in the plane of the spindle speed Ω and the tool path s are presented in the superchart.

The case studies show that the favorable parameter domains are located at the resonant spindle speeds from the viewpoint of

stability. It is also shown that the Maximum Surface Location Errors can be substantial at these spindle speeds. However, if the trivial or the non-trivial appropriate axial immersion are applied, then good surface quality can be achieved even for resonant spindle speeds. The numerical and the experimental case studies shows good agreement, which validates the theoretical results.

ACKNOWLEDGMENT

This paper was supported by the Hungarian Scientific Research Fund - OTKA PD-112983 and the Janos Bolyai Research Scholarship of the Hungarian Academy of Sciences. The research leading to these results has received funding from the European Research Council under the European Unions Seventh Framework Programme (FP/2007-2013) / ERC Advanced Grant Agreement n. 340889.

REFERENCES

- [1] Tlustý, J., and Spacek, L., 1954. *Self-excited vibrations on machine tools*. Nakl. CSAV, Prague. in Czech.
- [2] Tobias, S., 1965. *Machine-tool Vibration*. Blackie, Glasgow.
- [3] Stepan, G., 1989. “Retarded dynamical systems: stability and characteristic functions”. *Longman Scientific and Technical*.
- [4] Insperger, T., J. Gradisek, M. Kalveram, G. S. K. W., and Govekar, E., 2006. “Machine tool chatter and surface location error in milling processes”. *Journal of Manufacturing Science and Engineering*, **128**, pp. 913–920.
- [5] Bachrathy, D., Insperger, T., and Stepan, G., 2009. “Surface properties of the machined workpiece for helical mills”. *Machining Science and Technology*, **13**(2), pp. 227–245.
- [6] Insperger, T., and Stepan, G., 2011. *Semi-discretization for time-delay systems*, Vol. 178. Springer, New York.
- [7] Butcher, E. A., Bobrenkov, O. A., Bueler, E., and Nindurjarla, P., 2009. “Analysis of milling stability by the chebyshev collocation method: algorithm and optimal stable immersion levels”. *Journal of Computational and Nonlinear Dynamics - ASME*, **4**, p. 031003.
- [8] Khasawneh, F. A., and Mann, B. P., 2011. “A spectral element approach for the stability of delay systems”. *International Journal for Numerical Methods in Engineering*, **87**, p. 566952.
- [9] Altintas, Y., and Budak, E., 1995. “Analytical prediction of stability lobes in milling”. *CIRP Annals - Manufacturing Technology*, **44**, pp. 357–362.
- [10] Budak, E., and Altintas, Y., 1998. “Analytical prediction of chatter stability in milling, part i: General formulation”. *Journal of Dynamic Systems Measurement and Control - ASME*, **120**, pp. 22–30.
- [11] Bachrathy, D., and Stepan, G., 2013. “Improved prediction of stability lobes with extended multi frequency solution”. *CIRP Annals - Manufacturing Technology*, **62**, pp. 411–414.
- [12] Altintas, Y., 2012. *Manufacturing Automation; Metal Cutting Mechanics, Machine Tool Vibrations, and CNC Design, 2nd Edition*. Cambridge University Press.
- [13] Bachrathy, D., Munoa, J., and Stepan, G., 2015. “Experimental validation of appropriate axial immersions for helical mills”. *The International Journal of Advanced Manufacturing Technology*, pp. 1–8.
- [14] Dombovari, Z., Barton, D. A., Wilson, R., and Stepan, G., 2010. “On the global dynamics of chatter in the orthogonal cutting model”. *International Journal of Non-Linear Mechanics*, **46**, pp. 330–341.
- [15] Budak, E., Altintas, Y., and Armarego, E. J. A., 1996. “Prediction of milling force coefficients from orthogonal cutting data”. *Journal of Manufacturing Science and Engineering*, **118**(2), pp. 216–224.
- [16] Dombovari, Z., Munoa, J., and Stepan, G., 2012. “General milling stability model for cylindrical tools”. In 3rd CIRP Conference on Process Machine Interactions (3rd PMI), Elsevier, Procedia CIRP 4, pp. 90–97.
- [17] Insperger, T., and Stepan, G., 2002. “Semi-discretization method for delayed systems”. *International Journal for Numerical Methods in Engineering*, **55**, pp. 503–518.
- [18] Ewins, D. J., 2000. *Modal Testing, Theory, Practice, and Application*. Research Studies Press 2nd edition.
- [19] Hajdu, D., Insperger, T., and Stepan, G., 2015. “The effect of non-symmetric frf on machining: A case study”. In ASME IDETC.
- [20] Bachrathy, D., and Stepan, G., 2012. “Bisection method in higher dimensions and the efficiency number”. *Periodica Polytechnica-Mechanical Engineering*, **56**(2), pp. 81–86.
- [21] Zapata, R., DeMarco, C., and Schmitz, T., 2008. “The milling dynamics super diagram: Combining stability and surface location error”. In Proceedings of American Society for Precision Engineering Annual Meeting.